# Carboxylic acids in clouds at a high-elevation forested site in central Virginia

# Carboxylic acids in clouds at a high-elevation forested site in central Virginia

William C. Keene,[1] Byard W. Mosher,[2] Daniel J. Jacob,[3] J. William Munger,[3] Robert W. Talbot,[2] Richard S. Artz,[4] John R. Maben,[1] Bruce C. Daube,[3] and James N. Galloway[1]

**Abstract.** During September 1990 we sampled coarse (>18-μm diameter) and fine (18- to 5.5-μm diameter) droplets and liquid-water content (LWC) in cloud from a tower on a forested ridge top in Shenandoah National Park, Virginia. Cloud-water pH and aqueous- and vapor-phase concentrations of carboxylic acids (HCOOH and $CH_3COOH$) and formaldehyde (HCHO) were measured in parallel over 1- to 1.5-hour intervals. Both size fractions of cloud droplets contained similar concentrations of carboxylic species and $H^+$ during most sampling; most cloud water was in coarse droplets. The pH of coarse (3.27-4.76) and fine (3.22-4.70) droplets coupled with total LWC of 0.04-0.56 g $m^{-3}$ STP (standard $m^3$ at $0°$ C and 1 atm) resulted in the partitioning of carboxylic acids primarily in the vapor phase. The observed phase partitioning for $CH_3COOH$ was within the uncertainty range of thermodynamic data. However, HCOOH exhibited significant phase disequilibria, which could not be explained by artifacts from variable LWC or from mixing droplets of different acidities. We hypothesize that the large volume of liquid water deposited on the forest canopy interacted with the near-surface cloud leading to apparent disequilibria based on time-integrated samples. HCOOH was selectively depleted relative to $CH_3COOH$ in cloud, particularly at higher pH, suggesting rapid removal of HCOOH by cloud-water deposition. We saw no evidence for significant production of HCOOH from the aqueous-phase oxidation of HCHO.

## 1. Introduction

Carboxylic acids are ubiquitous chemical constituents of the global troposphere that contribute significantly to the acidity of precipitation and cloud water, especially in regions far from anthropogenic influences [e.g., *Keene and Galloway*, 1988]. There are many carboxylic acids in the troposphere, but HCOOH and $CH_3COOH$ are typically in the highest concentrations [e.g., *Keene et al.*, 1983]. Various sources for atmospheric HCOOH and $CH_3COOH$ have been hypothesized, including gas-phase oxidation of precursor organic compounds [*Jacob and Wofsy*, 1988; *Galloway et al.*, 1989; *Madronich and Calvert*, 1990; *Moody et al.*, 1991]; direct emission from plants [*Talbot et al.*, 1990], soils [*Sanhueza and Andreae*, 1991] and formicine ants [*Graedel and Eisner*, 1988]; and fossil-fuel and biomass combustion [*Kawamura et al.*, 1985; *Talbot et al.*, 1988]. Aqueous-phase chemistry in clouds provides either a source or a sink for HCOOH [*Chameides and Davis*, 1983; *Jacob*, 1986] but is thought to have little effect on $CH_3COOH$ [*Jacob and Wofsy*, 1988].

Wet and dry deposition are the primary atmospheric sinks for HCOOH and $CH_3COOH$ [*Sanhueza et al.*, 1992]; gas-phase oxidation by OH is slow [*Atkinson*, 1990].

Several field studies have investigated multiphase chemical processes involving HCOOH and $CH_3COOH$ in clouds and fogs [e.g., *Winiwarter et al.*, 1988, 1992; *Facchini et al.*, 1992; *Sanhueza et al.*, 1992]. Concentrations of HCOOH and $CH_3COOH$ measured simultaneously in the vapor phase and in bulk cloud water or fog water often diverge significantly from those based on thermodynamic properties, especially at pH greater than 5. Observed disequilibria between phases have been attributed to organic films on droplets that limit mass transfer [*Facchini et al.*, 1992] and to artifacts resulting when droplets with different acidities mix [*Pandis and Seinfeld*, 1991] or LWC changes during sampling [*Winiwarter et al.*, 1992; *Pandis and Seinfeld*, 1992]. These studies also report no evidence for pH-dependent, aqueous-phase production or destruction of HCOOH as modeled by *Chameides and Davis* [1983] and *Jacob* [1986]. Several studies suggest that clouds may be a net sink for tropospheric HCOOH [*Jacob and Wofsy*, 1988; *Sanhueza et al.*, 1991].

The Shenandoah Cloud and Photochemistry Experiment (SCAPE) investigated tropospheric oxidative processes and, in particular, the chemical dynamics of carboxylic acids and carbonyl compounds in surface air at a forested ridge top in central Virginia during September 1990. In this paper we have analyzed the subset of SCAPE data generated during cloud events (1) to assess the size dependence of droplet composition and its influence on phase partitioning of carboxylic acids and (2) to investigate physiochemical

---

[1]Department of Environmental Sciences, Clark Hall, University of Virginia, Charlottesville.

[2]Institute for the Study of Earth, Oceans, and Space, University of New Hampshire, Durham.

[3]Division of Applied Sciences and Department of Earth and Planetary Sciences, Harvard University, Cambridge, Massachusetts.

[4]Air Resources Laboratory, National Oceanic and Atmospheric Administration, Silver Spring, Maryland.

processes controlling in-cloud concentrations of carboxylic acids.

## 2. Methods

### 2.1. Site Description

We sampled cloud water and trace gases from a 15-m tower on a mountain ridge at Pinnacles (1037-m elevation) in the north central section of Shenandoah National Park (SNP), Virginia (38° 37' N, 78° 21'W). The top of the tower was 3 m above the surrounding forest canopy. Samples were processed in a field laboratory approximately 250 m from the tower. The sampling site was at the upper boundary of the Shaver Hollow watershed within the Appalachian oak eco-region [*Bailey*, 1978]. The second-growth forest was dominated by chestnut oak (*Quercus prinus*) and northern red oak (*Quercus rubra*) that collectively comprised 65% of the total biomass [*Harrison and Shugart*, 1990].

### 2.2. Sampling and Analytical Techniques

**2.2.1. Chemical composition of cloud water.** Coarse (>18-μm diameter) and fine (18- to 5.5-μm diameter) cloud droplets were separately sampled over 1.0- to 1.5-hour intervals with an active strand collector equipped with a fractionating inlet [*Munger et al.*, this issue). The collector was mounted on a retractable mast approximately 2.5 m above the top of the tower and the inlet was turned into the wind during sampling. Before each event, precleaned cartridges of Teflon strands for the fine stage were installed and the sampler was thoroughly rinsed with approximately 10 L of type 1 (>18.3 MΩ cm$^{-1}$) deionized water (DIW) sprayed through the inlet from a pressurized polyethylene container. Conductivities of the final rinse water from each stage were measured to verify cleanliness. After rinsing, ambient cloud water was sampled for 0.5 to 1.0 hour (depending on LWC) to thoroughly wet and flush the collector before any samples were kept for chemical analysis. The collector was thoroughly rinsed with DIW after each event and then wrapped with polyethylene film to prevent contamination.

Immediately after collection, cloud-water samples were weighed, analyzed for pH and conductivity [*Galloway et al.*, 1982], and divided into two aliquots. Aliquot 1 was treated with 500 μL of CHCl$_3$ to prevent microbial degradation [*Keene et al.*, 1983], stored in the dark at 4° C, and transferred to the University of Virginia (UVA) for further analysis. HCOOH$_t$ (HCOOH$_{aq}$ + HCOO$^-$) and CH$_3$COOH$_t$ (CH$_3$COOH$_{aq}$ + CH$_3$COO$^-$) were measured by ion-exclusion chromatography using procedures described by *Keene et al.* [1989] for UVA. SO$_4^{2-}$, NO$_3^-$, and Cl$^-$ were measured by ion chromatography (IC) using Dionex AG4, AS4, and AMMS columns and an isocratic 4.0 mM Na$_2$CO$_3$ eluent. NH$_4^+$ was measured by automated colorimetry and Ca$^{2+}$, Mg$^{2+}$, Na$^+$, and K$^+$ by atomic-absorption spectroscopy [*Galloway et al.*, 1982]. Data quality was verified by assessing ion balances, analyzing lab and field splits, intercomparing with laboratories at the University of New

Hampshire and elsewhere, and analyzing audit solutions provided by the U.S. Environmental Protection Agency and the National Institute of Standards and Technology. Analytical data were unbiased and precise to approximately ±5%.

In the second aliquot, carbonyls were derivatized using 2,4-dinitrophenylhydrazine (2,4-DNPH) and then analyzed by reverse-phase, high-performance liquid chromatography (HPLC); overall measurement uncertainties for HCHO were about 20% [*Munger et al.*, this issue]. Any S(IV) adducts in the cloud water did not decompose at the low pH used for derivatization and thus were not analyzed.

**2.2.2. Liquid water content.** LWC was independently measured by two techniques. Technique 1 used a LWC-sampling device described by *Valente et al.* [1989]. Cloud droplets were removed from the airstream by impacting a flow-through polypropylene mesh cartridge. The inlet nozzle upstream of the cartridge was positioned into the wind and flow rates were manually adjusted based on wind velocity to maintain isokinetic flow. We weighed the water collected in the cartridge and calculated LWC of the cloud based on the volume of sampled air. Technique 2 involved estimating LWC for each size fraction of droplets from the corresponding volume of water sampled by the cloud-water collector, the volume of air processed through the collector, and the theoretical collection efficiencies of the rods and strands [see *Munger et al.*, this issue].

Paired data generated by the two techniques typically agreed within about ±5% or ±0.03 g m$^{-3}$ STP for sampling intervals during which clouds were continuously present [*Munger et al.*, this issue]. LWC reported here corresponded to those estimated using the cloud-water collector since it allowed LWC for the two size fractions of droplets to be quantified.

**2.2.3. Interstitial gases.** Interstitial carboxylic and carbonyl gases were sampled over the same time intervals as cloud water. An inertial separator to remove droplets and coarse aerosol (> 1-μm diameter) from the sample air [*Munger et al.*, this issue] was positioned upstream of the gas samplers. HCOOH$_{(g)}$ and CH$_3$COOH$_{(g)}$ were sampled in DIW-filled mist chambers and analyzed by IC; overall measurement uncertainties were 10-15% [*Talbot et al.*, this issue]. Carbonyls were sampled in 2,4-DNPH-filled mist chambers and analyzed by HPLC; overall measurement uncertainties for HCHO were about 25% [*Munger et al.*, this issue].

**2.2.4. Chemical composition of precipitation.** During cloud events, precipitation was sampled sequentially from the top of the tower using 27.9-cm-diameter, high-density polyethylene funnels threaded onto 2-L, high-density polyethylene bottles [*Galloway et al.*, 1982]. The collectors were mounted in an anodized aluminum bracket attached to an outrig boom on the windward side. We exposed a clean precipitation collector at the beginning of each event and checked it at the end of each cloud sampling. When enough precipitation for complete analysis (about 60 mL) had been collected, the sample was recovered and a clean funnel and bottle installed. Samples were then processed and analyzed following the same procedures used for cloud water;

measurement uncertainties were the same as those for cloud water (section 2.2.1).

**2.2.5. Site meteorology and transport.** Temperature, relative humidity, barometric pressure, and wind speed and direction were continuously measured from the top of the tower using instruments and data-acquisition equipment provided by the Mountain Cloud Chemistry Project (MCCP) [*Gilliam et al.*, 1989]. Three-dimensional back trajectories for air parcels associated with cloud events were calculated using the NOAA HYbrid Single-particle Lagrangian Integrated Trajectories (HY-SPLIT) model [*Draxler*, 1992; *Rolph*, 1992, 1993]. The data used to calculate SCAPE trajectories had spatial and temporal resolutions of 180 km and 2 hours, respectively. The model included 10 sigma layers (terrain-following coordinates) in the bottom 600 mbars of the atmosphere; the lowest layer was approximately 200 m above the surface. Simulations were typically reliable for 2 or 3 days and were usually reasonable indicators of air-parcel origins for several more days.

# 3. Results and Discussion

## 3.1. Cloud Events Sampled

We sampled five discrete cloud events during September 1990; three (September 20, 22, and 30) were relatively short (<5 hours) and associated with occasional cloud breaks. Paired measurements of LWC diverged significantly during cloud breaks suggesting differential rates of evaporation in the samplers. Because evaporation would bias concentrations of chemical species in cloud water, data corresponding to intervals of broken clouds were suspect. Therefore only data for the two events with the longest periods of continuous cloud were analyzed in detail.

Cloud event 1 was generated when a cool continental polar air mass from Canada encountered maritime tropical air as it penetrated into the central Atlantic region. The sampled air parcel flowed to the site off the Atlantic Ocean as indicated by trajectories following a front that wrapped around the Canadian air mass (Figure 1a). The cloud was thus generated in relatively clean Canadian air modified by 2 to 3 days over the ocean. Continuous cloud enveloped the site at approximately 1845 eastern daylight time (EDT) on September 8 and cloud sampling started at 2005 (EDT). Intermittent drizzle fell during the first half of the event but then stopped (Table 1). A total of 0.21 cm of precipitation was recorded in the rain gauge during sampling (Table 2). Temperatures, barometric pressures, and wind velocities are summarized in Table 1. There were occasional breaks in the cloud during the last sampling interval, which started at 1405 (EDT) and stopped at 1530 (EDT) on September 9.

Compared to polluted clouds typical of the region [e.g., *Weathers et al.*, 1988], event 1 was unusually clean, reflecting its source over central Canada and possibly other factors such as washout during transport. During the middle of the event, pH for both fractions of cloud water ranged from 4.5 to 4.8 (Figure 2b), specific conductance ranged from 10 to 15 $\mu$S cm$^{-1}$, and ionic strengths were in the range of those for precipitation in remote continental regions [e.g., *Galloway et al.*, 1982].
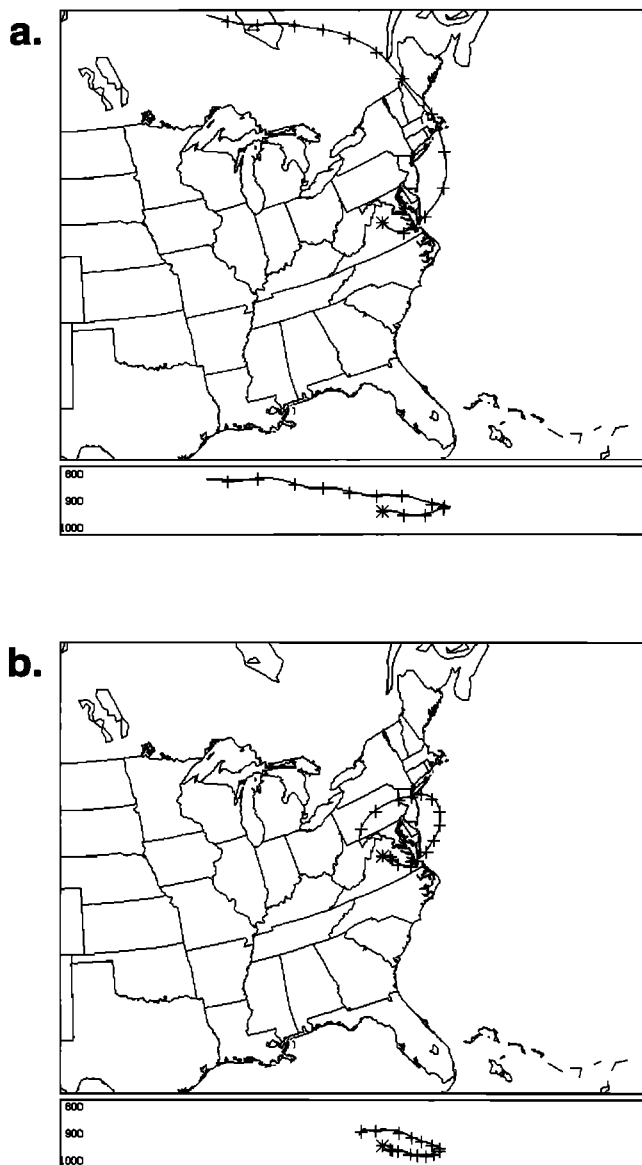
**Figure 1.** Air-parcel back trajectories for the cloud events. Tic marks indicate every 12 hours and calculations were carried out to a maximum of 10 days. Units for vertical axes are millibars. (a) 1200 UT, September 9, 1990 (event 1). (b) 2000 UT, September 13, 1990 (event 2).

Cloud event 2 was associated with a somewhat weaker intrusion of continental polar air that penetrated only into southern Pennsylvania where the cold front stalled, weakened, and finally dissipated. A slower trajectory was associated with this more stagnant air mass (Figure 1b). Although flow was off the Atlantic Ocean during much of the period, the trajectory remained either over the heavily populated middle Atlantic region or near the shore throughout the 10 days. Continuous cloud was sampled from 0646 to 2330 (EDT) on September 13. Intermittent showers during the first half of the event produced 0.98 cm of precipitation (Tables 1 and 2). Event 2 was significantly more acidic than event 1 (e.g., Figures 2b and 2h) during most sampling.

**Table 1.** Meteorological Conditions During
Each Sampling Interval

| Mid-point[a], EDT | Average | | | |
|---|---|---|---|---|
| | Temp-erature, °C | Pres-sure, mbar | Wind Speed, m s$^{-1}$ | Rain[b] |
| *Event 1, September 8-9, 1990* | | | | |
| 2039 | 14.5 | 844.2 | 6.1 | N/D |
| 2147 | 14.6 | 844.6 | 6.3 | D |
| 2255 | 14.3 | 844.7 | 7.3 | D |
| 0003 | 13.9 | 844.6 | 7.8 | D |
| 0111 | 13.6 | 844.5 | 7.7 | D/N |
| 0219 | 13.6 | 844.2 | 7.6 | N |
| 0328 | 13.5 | 844.2 | 8.1 | N/D |
| 0436 | 13.4 | 843.9 | 8.8 | D |
| 0543 | 13.2 | 843.8 | 9.6 | D |
| 0650 | 13.1 | 843.8 | 9.9 | N |
| 0757 | 13.1 | 844.0 | 8.7 | N |
| 0912 | 13.3 | 844.0 | 7.8 | N |
| 1026 | 13.8 | 844.0 | 6.7 | N |
| 1146 | 14.4 | 843.9 | 4.7 | N |
| 1319 | 16.1 | 843.7 | 2.5 | N |
| 1448 | 17.4 | 843.4 | 1.7 | N |
| *Event 2, September 13, 1990* | | | | |
| 0719 | 15.8 | 845.1 | 3.9 | N |
| 0825 | 15.3 | 845.1 | 4.5 | S |
| 0933 | 15.0 | 845.3 | 4.2 | S |
| 1050 | 15.5 | 845.4 | 4.2 | S/N |
| 1218 | 15.8 | 845.4 | 3.9 | N/S |
| 1350 | 15.9 | 845.3 | 3.9 | S/N |
| 1523 | 15.8 | 844.9 | 4.7 | S |
| 1655 | 15.7 | 844.6 | 5.4 | S |
| 1830 | 15.7 | 844.4 | 6.5 | D |
| 1956 | 15.0 | 844.2 | 7.4 | D/N |
| 2121 | 14.8 | 844.3 | 6.4 | N |
| 2250 | 15.4 | 844.4 | 3.7 | N |

[a]Corresponds to the midpoint for each sampling interval.
[b]Rain observed as (S) showers or (D) drizzle; (N) no rain present.

### 3.2. Droplet-Size-Dependent Variability in LWC and Solute Concentrations

LWC varied considerably over time during each event (Figures 2a and 2g). Most cloud water was in coarse droplets and the greatest absolute and relative temporal variabilities were in the coarse fraction. LWC of fine-fraction droplets was relatively constant from one sample to the next. The presence of drizzle (Table 1) coincided with variability in LWC (Figure 2a) during event 1 indicating that some drizzle may have been sampled as coarse-fraction cloud water. The chemical compositions of cloud water (Figures 2b, 2c, 2d) and of precipitation (Table 2) during

these periods of drizzle were similar, however, and thus would have little influence on thermodynamic equilibria.

In contrast to the typically large size-dependent differences in LWC, pH and concentrations of $HCOOH_t$ and $CH_3COOH_t$ in the two fractions of cloud water were similar during most sampling (Figure 2). Of the three, pH varied the most between droplet sizes particularly during the first half of event 2 when acidities (primarily $H_2SO_4$ and $HNO_3$) of the fine fraction occasionally exceeded those of the coarse by factors of 2 or more (Figure 2h). Splash from the intermittent showers during this period (Tables 1 and 2) may have diluted coarse-fraction cloud water thereby contributing to these differences. Acidity of the precipitation (Table 2) was substantially lower than that of the corresponding cloud water (Figure 2h) although $HCOOH_t$ and $CH_3COOH_t$ concentrations were similar (Table 2, Figure 2). During most intervals, however, size-dependent differences in concentrations of $H^+$ and the carboxylic species were <25% and often statistically indistinguishable. *Munger et al.* [1989] also report similar concentrations of $H^+$ and carboxylic species in different size fractions of marine-stratus-cloud droplets despite large size-dependent variabilities in concentrations of other solutes.

### 3.3. Phase Partitioning and Thermodynamic Relationships

Phase-partitioning equilibria for HCOOH and $CH_3COOH$ in clouds are controlled by Henry's law constants ($K_H$) and dissociation constants ($K_a$) for each acid, pH and ionic strength of cloud water, LWC, temperature, and pressure [e.g., *Clegg and Brimblecombe*, 1990]. For the cloud conditions that we sampled (pH <4.8 and LWC <0.6 g m$^{-3}$ STP), both acids were primarily partitioned in the vapor phase (Figure 2). The measured vapor-phase fraction of HCOOH ranged from 62% to 98% of the total (aqueous plus vapor) and that of $CH_3COOH$ ranged from 88% to >98% of the total.

To account for the pH dependence of phase partitioning, vapor-aqueous equilibria for partially dissociated acids can be expressed as pseudo-Henry's law constants ($K_H^*$) [e.g., *Schwartz*, 1984].

$$K_H^* = \frac{[RCOOH_t]}{[RCOOH_g]} = \frac{[RCOOH_{aq}]}{[RCOOH_g]} * \left(1 + \frac{K_a}{[H^+]}\right)$$

$$= K_H * \left(1 + \frac{K_a}{[H^+]}\right) \qquad (1)$$

where $RCOOH_t$ is the total aqueous-phase concentration ($RCOOH_{aq}$ + $RCOO^-$) and $RCOOH_g$ is the corresponding vapor-phase mixing ratio at equilibrium. We calculated expected or theoretical $K_H^*$ (equation 1) for HCOOH and $CH_3COOH$ using $K_H$ (Table 3), $K_a$ (1.772 x 10$^{-4}$ and 1.754 x 10$^{-5}$ M, respectively, at 25° C), and corresponding temperature corrections reported by *Clegg and Brimblecombe* [1990]. Published estimates of $K_H$ for HCOOH and $CH_3COOH$ vary considerably (Table 3) (also see *Johnson and Betterton* [1993]), however, indicating uncertainties in expected phase partitioning of a factor of 2 or more.

**Table 2.** In-Cloud Precipitation

| Time On, EDT | Time Off, EDT | Amount, cm | pH | HCOOH$_t$, $\mu$M | CH$_3$COOH$_t$, $\mu$M |
|---|---|---|---|---|---|
| *Event 1, September 8-9, 1990* | | | | | |
| 1905 | 0038 | 0.13 | 3.95 | 14.2 | 4.5 |
| 0038 | 1058 | 0.08 | 4.30 | 7.7 | 2.8 |
| *Event 2, September 13, 1990* | | | | | |
| 0657 | 0858 | 0.38 | 4.49 | 4.4 | 4.5 |
| 0858 | 1132 | 0.25 | 4.48 | 3.1 | 4.5 |
| 1132 | 1605 | 0.25 | 4.17 | 9.0 | 7.4 |
| 1605 | 0703 | 0.10 | 3.85 | 11.1 | 7.0 |

Observed $K_H^*$ ($K_{H\ obs}^*$) was calculated from concurrent vapor and aqueous measurements in cloud:

$$K_{H\ obs}^* = \frac{[RCOOH_t]}{[RCOOH_g]} \qquad (2)$$

Theoretical and observed $K_H^*$ for each acid were plotted as functions of pH in Figures 3a and 3b [e.g., *Winiwarter et al.*, 1988]. The theoretical $K_H^*$ curve corresponds to 288 K, the average temperature during events 1 and 2. For comparison we plotted experimental $K_H^*$ for cloud and fog water reported by other investigators [Winiwarter et al., 1988; *Facchini et al.*, 1992; *Sanhueza et al.*, 1992]. These combined data for HCOOH (Figure 3a) showed large departures from expected phase partitioning and, in particular, did not capture the expected $K_H^*$-versus-pH dependency. In contrast, CH$_3$COOH phase partitioning measured during SCAPE (Figure 3b) was typically within the ± 2 uncertainty factor for expected values inferred from Table 3. The small but systematic undersaturation (82% of observations) of cloud water relative to the gas phase suggests the possibility that the $K_H$ for CH$_3$COOH estimated by *Clegg and Brimblecombe* [1990] may overestimate the true value.

To assess these relationships further, we compared temporal variabilities in measured vapor-phase mixing ratios for each acid (HCOOH$_g$ and CH$_3$COOH$_g$) with corresponding variabilities in vapor-phase mixing ratios calculated to be in thermodynamic equilibrium with the measured concentrations in coarse- and fine-fraction cloud water (Figure 4). Such plots allowed us to compare thermodynamic relationships directly with relative variabilities in corresponding field measurements. During the middle of event 1, the aqueous and vapor phases for HCOOH partitioned as expected based on thermodynamic data, but during event 2 the two size fractions of droplets were alternately supersaturated and undersaturated relative to HCOOH$_g$. Equilibria relationships for coarse and fine droplets also diverged during the middle of event 2 possibly because chemically distinct precipitation diluted coarse-fraction cloud water (see section 3.2).

### 3.4. Possible Explanations for Disequilibria Between Phases

#### 3.4.1. Sampling artifacts.
If a cloud parcel contains droplets of different pH in thermodynamic equilibrium with the gas phase and the droplets are mixed when sampled, partially dissociated acids in the bulk solution will be supersaturated relative to the original atmosphere [*Pandis and Seinfeld*, 1991]. Similarly, if cloud-water acidity varies substantially during sampling, partially dissociated acids in the time-integrated sample will be supersaturated relative to the original atmosphere. These effects are most important when the pH of the bulk solution is greater than the pK$_a$ of the acid (i.e., when $K_H^*$ is strongly dependent on pH).

Variations in LWC during sampling can also lead to artifact undersaturation [*Winiwarter et al.*, 1992] or supersaturation [*Pandis and Seinfeld*, 1992] of bulk cloud-water samples relative to the original atmosphere. The magnitude of apparent disequilibria resulting from this effect is greatest when the pH of the bulk solution is greater than the corresponding pK$_a$ of the acid and LWC varies substantially over the sampling interval.

The pH of virtually all cloud water we sampled (Figures 2b and 2h) was less than the pK$_a$ for CH$_3$COOH (4.76 at 25° C), thus variations in droplet pH and in LWC during sampling could not explain the small but systematic disequilibria for CH$_3$COOH. Supersaturation of HCOOH in cloud water was most frequent at pH less than the pK$_a$ of HCOOH (3.75 at 25° C) (Figure 3). Because such sampling artifacts as those described above would only have had a minor influence in this pH range, we concluded that other processes contributed to this apparent supersaturation. During the middle of event 1, both cloud-water fractions were in equilibrium with HCOOH$_g$ (Figure 4a) despite substantial variability in LWC (Figure 2a) and high cloud-water pH (Figure 2b) relative to the pK$_a$ for HCOOH. Compared to all sampling intervals during the entire experiment, sampling artifacts associated with LWC variability should have been greatest under these conditions.
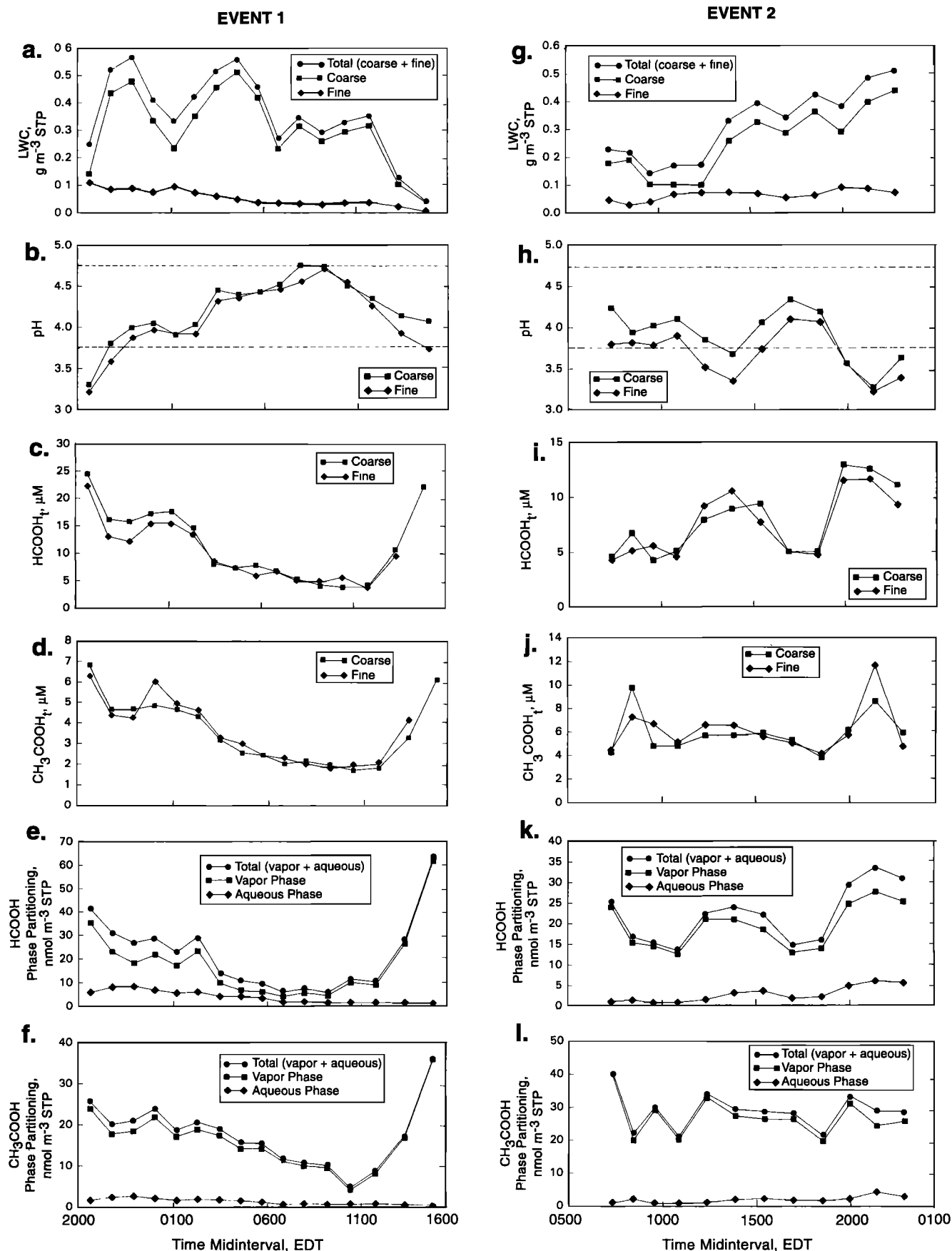
**Figure 2.** Physical and chemical characteristics of cloud events. (a) and (g) Liquid water content (LWC) for events 1 and 2, respectively. (b) and (h) pH for events 1 and 2, respectively; $pK_a$ lines for HCOOH (3.75) and $CH_3COOH$ (4.76) are indicated. (c) and (i) $HCOOH_t$ ($HCOOH_{aq}$ + $HCOO^-$) for events 1 and 2, respectively. (d) and (j) $CH_3COOH_t$ ($CH_3COOH_{aq}$ + $CH_3COO^-$) for events 1 and 2, respectively. (e) and (k) Measured phase partitioning of HCOOH for events 1 and 2, respectively. (f) and (l) Measured phase partitioning of $CH_3COOH$ for events 1 and 2, respectively.

**Table 3.** Reported Henry's Law Constants for HCOOH and CH₃COOH

| $K_H \cdot 10^3$, M atm⁻¹ | Delta H, kJ mol⁻¹ | Method[a] | References |
|---|---|---|---|
| | | *HCCOH* | |
| 7.5 | -22 | exp | *Johnson and Betterton* [1993][b] |
| 3.6 | | calc | *Betterton* [1992] |
| 13.4[c] | | exp | *Servant et al.* [1991] |
| 10.3[c] | | exp | *Servant et al.* [1991] |
| 5.7[c] | | exp | *Servant et al.* [1991] |
| 5.2[d] | | model | *Clegg and Brimblecombe* [1990] |
| 5.39 | | calc | *Clegg and Brimblecombe* [1990][e] |
| 5.6 | | calc | *Keene and Galloway* [1986][f] |
| 3.7 | -47.4 | calc | *Chameides and Davis* [1983][g] |
| | | *CH₃COOH* | |
| 3.1 | -37 | exp | *Johnson and Betterton* [1993][b] |
| 9.3[h] | | exp | *Servant et al.* [1991] |
| 11.2[h] | | exp | *Servant et al.* [1991] |
| 6.4[h] | | exp | *Servant et al.* [1991] |
| 5.24[d] | | model | *Clegg and Brimblecombe* [1990] |
| 8.61 | | calc | *Clegg and Brimblecombe* [1990][e] |
| 8.8 | -54 | calc | *Jacob et al.* [1989][i] |
| 8.8 | | calc | *Keene and Galloway* [1986][f] |

Unless otherwise noted, data correspond to 25° C.

[a]Measured experimentally (exp), modeled from partial pressure data (model), or calculated empirically from thermochemical data (calc).

[b]Paper has been accepted pending revision; $K_H$ values are tentative and may be revised; aqueous concentration = $2.5 \cdot 10^{-3}$ M; ionic strength = 0.01.

[c]Determined for aqueous concentrations of $2.7 \cdot 10^{-5}$ M, $2.7 \cdot 10^{-4}$ M, and 2.7 M, respectively; temperature = 24° C; ionic strength = 0.01.

[d]Explicit temperature corrections reported.

[e]Using data reported by *Wagman et al.* [1982].

[f]Using data reported by *Wagman et al.* [1965b] and *Chao and Zwolinski* [1978].

[g]Using data reported by *Wagman et al.* [1965a] and *Weast* [1979].

[h]Determined for aqueous concentrations of $1.8 \cdot 10^{-5}$ M, $1.8 \cdot 10^{-4}$, and 1.8 M, respectively; temperature = 23° C; ionic strength = 0.01.

[i]Using data reported by *Wagman et al.* [1982] and *Chao and Zwolinski* [1978].

Since we found no large deviations, we concluded that variations in LWC during sampling probably did not account for artifact undersaturation or supersaturation of HCOOH. Other processes probably contributed to the apparent disequilibria in our data.

**3.4.2. Influence of canopy water.** In the absence of precipitation, cloud water at Pinnacles during the growing season deposits at an average rate of about 0.02 cm h⁻¹ (0.2 L m⁻² h⁻¹) [*Sigmon et al.*, 1989; J. T. Sigmon, Duke University, unpublished data, 1992]. The average LWC of clouds at the site is 0.18 g m⁻³ STP (J. T. Sigmon, Duke University, unpublished data, 1992), and thus the average volume of cloud water deposited per hour corresponds to the average liquid water in about $10^3$ m³ STP of cloud. This deposition rate suggests, however, that a larger volume of cloud interacts with the canopy each hour since canopy-collection efficiencies for cloud water normally range from <0.05 to 0.3 [e.g., *Lovett*, 1984, 1988; *Joslin et al.*, 1990].

During the growing season, deciduous forest canopies typically incept and retain on the order of 1 to 3 mm (1 to 3 L m⁻²) of incident precipitation [e.g., see *Rutter et al.*, 1975; *Parker*, 1983, 1990, and references]. Assuming the canopy holds a similar amount of cloud water, this corresponds to the average liquid water in about $10^4$ m³ STP of cloud at the site. This water mass balance indicates that large volumes of cloud pass through and interact with the forest canopy during cloud events. Differences in topography, canopy geometry, and wind velocity contribute to the rapid rates of canopy ventilation inferred from these data (i.e., < 1 minute for a 10-m-deep canopy processing $10^3$ m⁻² h⁻¹ of cloud) relative to those estimated at other locations (i.e., 30 min during the day and 5 hours at night in the Amazon) [*Trumbore et al.*, 1990].

We hypothesize that this large volume of dispersed canopy water significantly influenced the chemical composition of near-surface clouds. Two liters per square meter of canopy
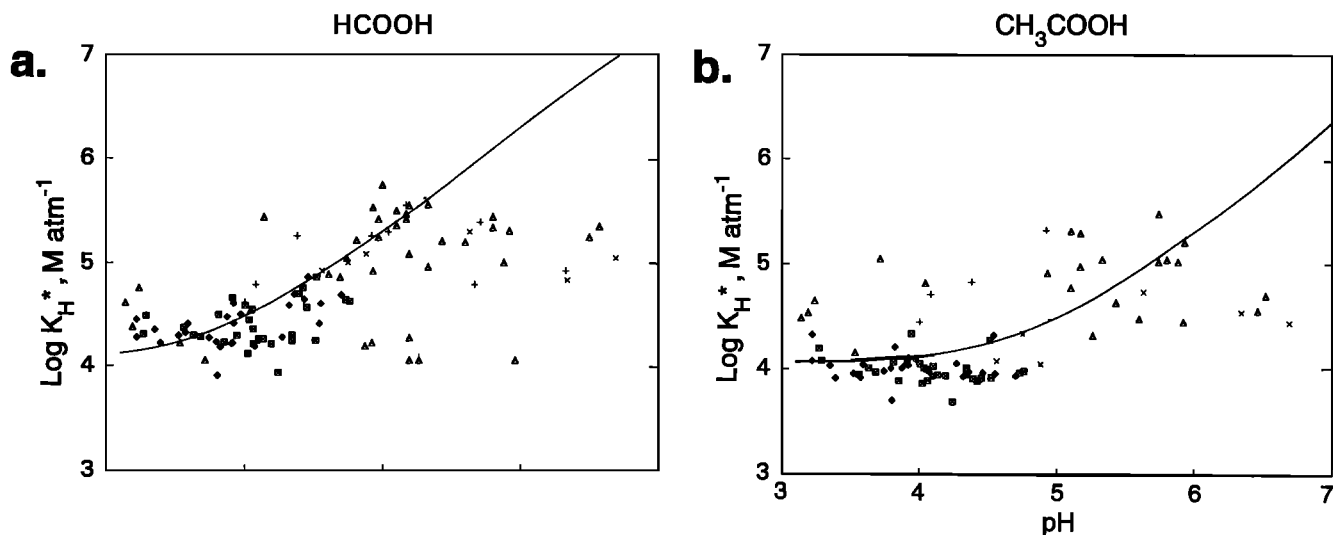
Figure 3. Pseudo-Henry's law constants for clouds and fogs as a function of pH. The line represents theoretical values at 288 K and symbols experimentally determined values at ambient temperatures (see text for calculation details). Squares correspond to coefficients for coarse droplets and diamonds to those for fine droplets calculated from SCAPE data; pluses are from *Winiwarter et al.* [1988], triangles from *Facchini et al.* [1992], and crosses from *Sanhueza et al.* [1992]. Temperature differences contribute to variability among the experimentally determined constants. (a) HCOOH. (b) $CH_3COOH$.

water uniformly distributed over the forest canopy (surface-area index of 5.4 [J. T. Sigmon, Duke University, unpublished data, 1992]; leaf-area index of 1.84 [*McIntyre et al.*, 1990]) corresponds to an aqueous film about 370-μm deep or about 10 to 20 times the median diameter of cloud droplets. Considerable variability in depth is expected since canopy water is not uniformly distributed but pools on leaves and in bark crevices. Canopy water should equilibrate slowly with cloud parcels because of the thick water layers and the large distances between gas molecules and canopy
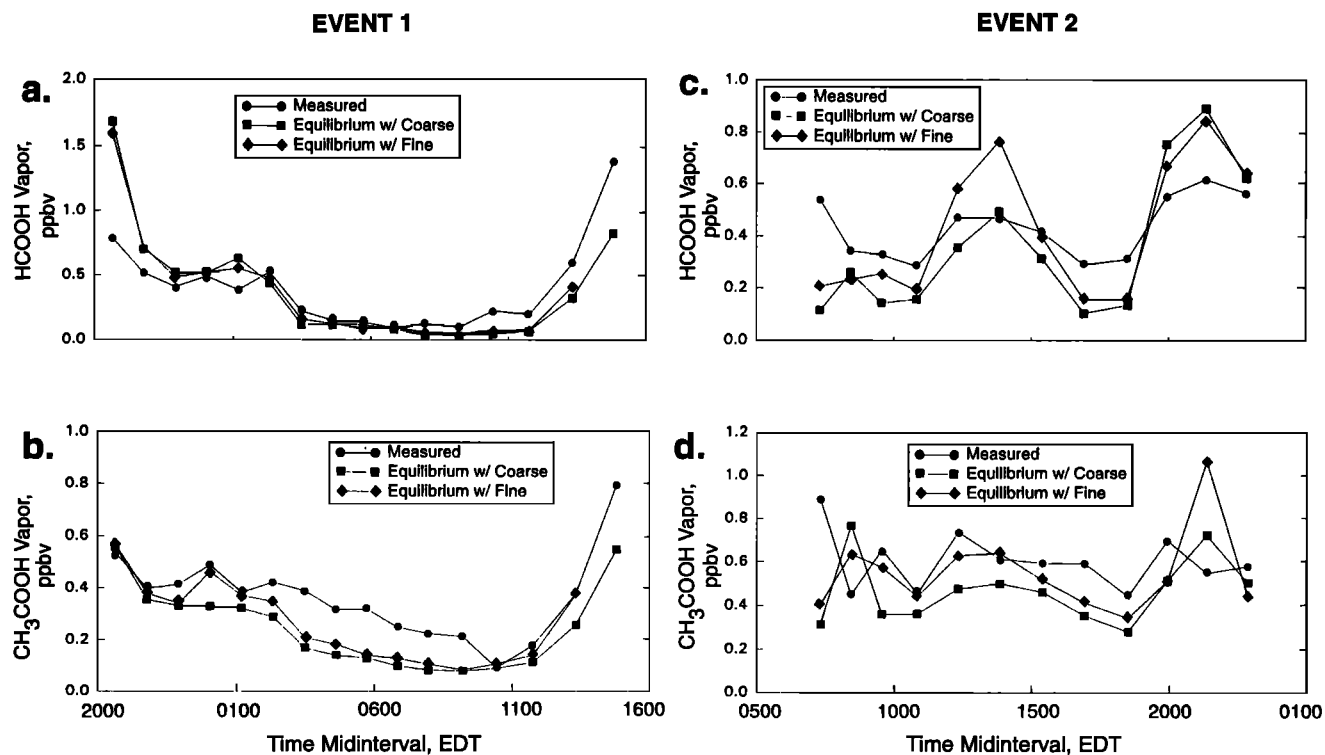


Figure 4. Measured vapor-phase mixing ratios (circles) compared with vapor-phase mixing ratios calculated to be in thermodynamic equilibrium with coarse-fraction cloud water (squares) and fine-fraction cloud water (diamonds). (a) and (c) HCOOH for events 1 and 2, respectively. (b) and (d) $CH_3COOH_t$ for events 1 and 2, respectively.

surfaces. Cloud water also deposits slowly relative to the total volume of canopy water (see above). Canopy water should, therefore, reflect some average of the past chemical composition of the cloud and thus equilibria exchange with canopy water should buffer temporal variability of carboxylic acids in cloud parcels passing through the canopy. The near-surface cloud that we sampled contained a mixture of parcels; some had interacted with the canopy, some had not. Since depositional losses had reduced the LWC of canopy-impacted parcels, time-integrated cloud water sampled immediately above the canopy was more heavily weighted by unimpacted parcels; gases sampled in parallel were equally weighted by impacted and unimpacted parcels.

For a cloud with chemistry that varied significantly over time, this mechanism predicts that variabilities in measured mixing ratios of carboxylic acid gases would be damped relative to those expected based on thermodynamic equilibria with the aqueous phase. HCOOH data for event 2, which exhibited highly variable chemistry (Figures 2h, 2i), followed this predicted pattern (Figure 4c). For a cloud with chemistry that did not vary significantly over time, no influence on apparent equilibria is expected since the composition of the canopy water and cloud water would be in equilibrium. During the middle of event 1, when cloud chemistry was fairly constant (Figures 2b and 2c), HCOOH was, as predicted, in thermodynamic equilibrium (Figure 4a). Our observations suggest that a rapidly ventilated forest canopy wetted by cloud water (dew or precipitation) could significantly influence the chemical composition of near-surface air.

Canopy effects may also have contributed to the apparent systematic undersaturation of aqueous $CH_3COOH$. If vegetation emitted $CH_3COOH$ directly [e.g., Talbot et al., 1990] or if canopy water leached $CH_3COOH$ from plant tissue, cloud parcels that interacted with the canopy would be enriched in $CH_3COOH$ (primarily as vapor at these cloud-water acidities) relative to unaffected cloud parcels. The LWC of canopy-impacted samples would also be reduced (see above). Canopy sources for $CH_3COOH$ could, therefore, lead to apparent undersaturation of the aqueous phase based on time-integrated cloud samples.

### 3.5. Aqueous Phase Production of HCOOH

Photochemical model simulations indicate that during the day HCOOH is produced in clouds by reaction of $HCHO_{aq}$ with $OH_{aq}$ and destroyed by reaction of $HCOO^-$ with $OH_{aq}$ [e.g., Chameides and Davis, 1983]. At pH < 5, HCOOH produced in the aqueous phase volatilizes to the gas phase where it has a long lifetime against oxidation; thus net production (production minus destruction) of HCOOH increases with decreasing pH down to about pH 3.5 [Jacob, 1986]. No pH-dependent controls for the concentrations of $CH_3CHOOH$ are known [Jacob and Wofsy, 1988]. Assuming there are no other sources of variability for the two acids, these studies suggest that total HCOOH in daytime clouds should increase relative to total $CH_3COOH$ as a function of $H^+$. From measured aqueous-phase concentrations of $H^+$, $HCOOH_t$, and $CH_3COOH_t$ in bulk

cloud water sampled in nonprecipitating clouds at the site, Keene and Galloway [1988] found that total HCOOH does increase relative to total $CH_3COOH$ in clouds as a function of $H^+$. These observations support the hypothesis that HCOOH is produced by aqueous-phase photochemistry. Substantial uncertainties were associated with that analysis, however, because LWC and vapor-phase mixing ratios of each acid in cloud were not measured directly and variability in ratios of $HCOOH_g$ to $CH_3COOH_g$ during noncloud periods at the site were not known.

We conducted a similar analysis using the more comprehensive data generated during this experiment. In the absence of surface clouds, $HCOOH_g$ and $CH_3COOH_g$ were highly correlated (slope = 2.78 parts per billion by volume (ppbv), intercept = -0.26 ppbv, $r^2$ = 0.88 [Talbot et al., this issue]), suggesting similar source and sink relationships for both acids throughout the region during SCAPE. Molar ratios of total HCOOH to total $CH_3COOH$ in events 1 and 2 (Figures 5a, 5c) were, however, lower than gas-phase ratios of the two acids in clear air suggesting that HCOOH was selectively depleted relative to $CH_3COOH$ in clouds. Although ratios of total HCOOH to $CH_3COOH$ increased as a function of cloud-water pH, similar relationships were observed during the day and at night (Figures 5a, 5c). Ratios of total HCOOH to $CH_3COOH$ reported by Keene and Galloway [1988] also vary as a function of pH during both day and night. Although not necessarily inconsistent with photochemical production or destruction of HCOOH in the aqueous phase, these relationships suggested that pH-dependent variabilities in ratios of total HCOOH to $CH_3COOH$ in clouds may have been primarily controlled by nonphotochemical processes.

One possible explanation relates to cloud-water deposition. Relative to total $CH_3COOH$, proportionately greater fractions of total HCOOH were partitioned in the aqueous phase of clouds (Figure 2). This pH-dependent phase partitioning must have led to proportionately more HCOOH being deposited via cloud water from near-surface clouds relative to $CH_3COOH$; the magnitude of difference between deposition rates must have varied directionally as a function of pH. The water mass balance (section 3.4.2) suggested substantial fluxes of cloud water to the canopy, and thus the potential existed for substantial pH-dependent fractionation between the two acids as a result of cloud-water deposition. Differential loss rates via cloud-water deposition would have been consistent with lower ratios of total HCOOH to $CH_3COOH$ in clouds relative to clear air, the apparent pH dependence of the in-cloud ratios, and the lack of an obvious diel influence on the pH dependence of the ratios.

Simulations of in-cloud photochemistry predict that the ratio of $HCOO^-$ to $HCHO_{aq}$ will approach a steady state defined by the oxidation of both species by $OH_{aq}$ [Chameides and Davis, 1983]. For the photochemical conditions during SCAPE, several hours would be required to reach steady state even in the middle of the day [Jacob, 1986]. Recently measured rate constants [Chin and Wine, 1993] suggest an equilibrium ratio of 0.25. During the night, ratios of $HCOO^-$ to $HCHO_{aq}$ would be expected to diverge from this equilibrium value as a result of other chemical or
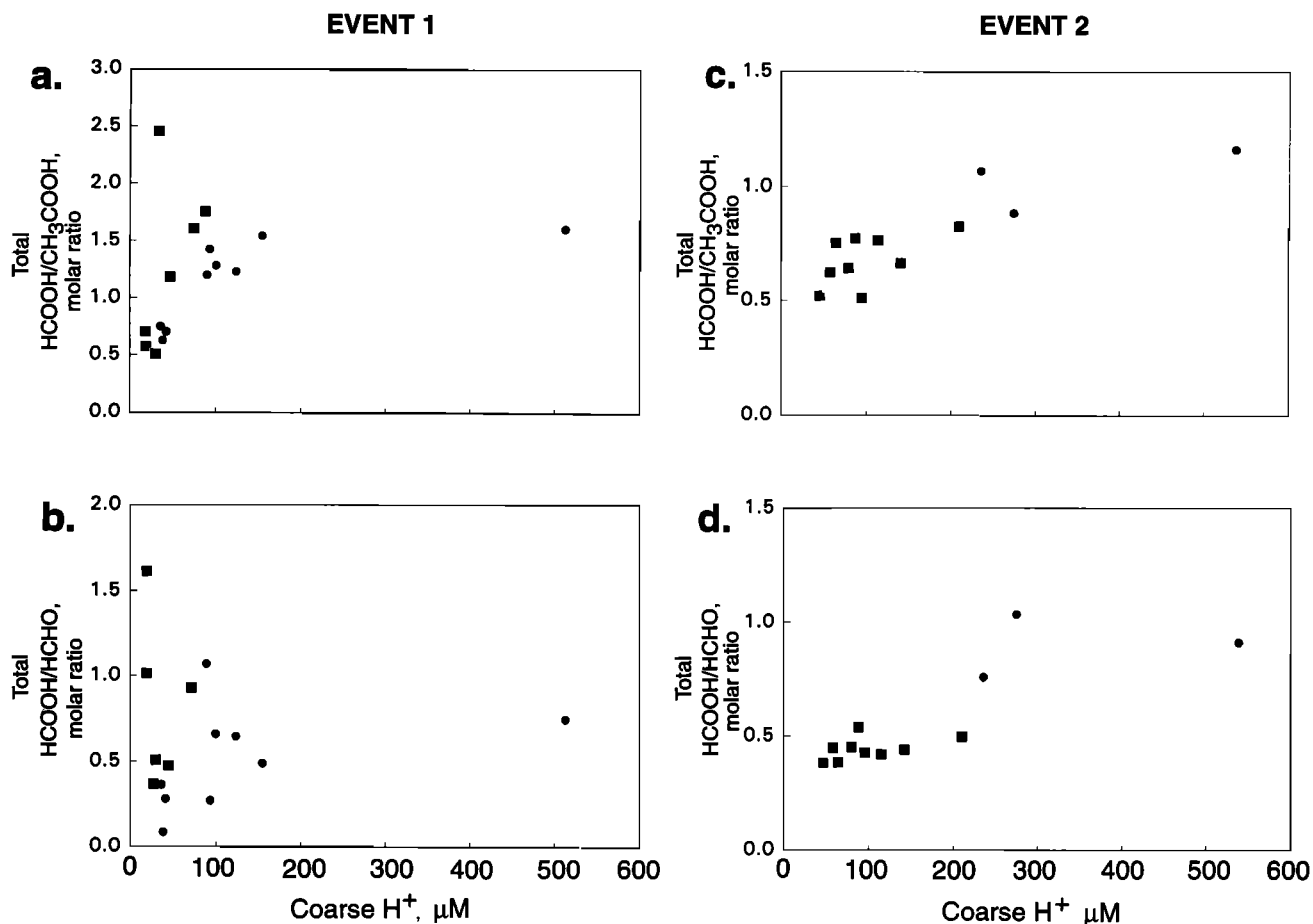
**Figure 5.** Ratios of total (vapor plus aqueous) HCOOH to $CH_3COOH$ versus coarse fraction $H^+$ for (a) event 1 and (c) event 2; ratios of total HCOOH to HCHO versus coarse fraction $H^+$ for (b) event 1 and (d) event 2. Squares indicate daytime values and circles nighttime values.

physical processes (e.g., differential rates of deposition). $HCOO^-$ to $HCHO_{aq}$ ratios during event 2 were similar to the predicted equilibrium value, but those during event 1 were 3 to 4 times higher (Table 4). No significant diel variability was observed in either case.

The pH dependence of the ratio of total HCOOH to HCHO was also examined for evidence of aqueous-phase chemistry. Assuming there were no other sources of variability for these species, higher concentrations of total HCOOH relative to total HCHO would be expected in more acidic clouds during the daytime if HCHO was oxidized to HCOOH via aqueous-phase chemistry. Daytime ratios did not appear to vary consistently as a function of $H^+$ during either event (Figures 5b, 5d).

Like those for most ground-based experiments, SCAPE data were generated within a Eulerian framework, yet questions concerning in-cloud chemical transformations are Lagrangian in nature. The processes that we investigated were somewhat obscured by transport, vertical mixing, and surface exchange, thus complicating data interpretation. Within the inherent uncertainties imposed by the experimental design, we saw no clear evidence that aqueous-phase oxidation of HCHO within clouds produced HCOOH. Processes other than this mechanism apparently dominated transformations involving these species in the near-surface clouds we sampled.

## 4. Conclusion

In-cloud measurements from SCAPE provided a unique data set with which to assess thermodynamic relationships and chemical transformations involving carboxylic acids and carbonyl compounds at a rural continental site. We sampled size-segregated droplets and interstitial gases in two cloud events during September 1990. LWC for coarse droplets ($>18$-$\mu m$ diameter) exhibited higher absolute concentrations and greater absolute and relative temporal variabilities than did fine droplets (18- to 5.5-$\mu m$ diameter). During most sampling, both size fractions of cloud droplets contained similar concentrations of carboxylic species and $H^+$. The pH of coarse (3.27-4.76) and fine (3.22-4.70) fraction cloud water coupled with total LWCs of 0.04-0.56 g m$^{-3}$ STP partitioned carboxylic acids primarily in the vapor phase. Measured phase partitioning for $CH_3COOH$ was within the uncertainty range of thermodynamic data. When temporal variability in cloud chemistry was low, phase partitioning for HCOOH also agreed with thermodynamic data; but when it was high, temporal changes in $HCOOH_g$ concentrations were damped relative to those expected based on thermodynamic equilibria with the aqueous phase. The disequilibria could not be explained by sampling artifacts resulting from mixing droplets of different acidities or variable LWC. We hypothesized that the large volume of liquid water deposited

**Table 4.** Summary of Molar Ratios for [HCOO⁻]/[HCHO$_{aq}$] in Clouds

| | Event 1, September 8-9, 1990 | | Event 2, September 13, 1990 | |
| --- | --- | --- | --- | --- |
| | Coarse Fraction | Fine Fraction | Coarse Fraction | Fine Fraction |
| *All Data* | | | | |
| Median | 1.23 | 1.07 | 0.32 | 0.20 |
| Arithmetic average | 1.28 | 1.09 | 0.34 | 0.29 |
| Standard deviation | 0.40 | 0.48 | 0.14 | 0.19 |
| Number of samples | 15 | 15 | 12 | 12 |
| *Daytime Only* | | | | |
| Median | 1.21 | 1.21 | 0.22 | 0.22 |
| Arithmetic average | 1.27 | 1.32 | 0.33 | 0.25 |
| Standard deviation | 0.31 | 0.50 | 0.13 | 0.11 |
| Number of samples | 6 | 6 | 9 | 9 |
| *Nighttime Only* | | | | |
| Median | 1.25 | 0.93 | 0.36 | 0.19 |
| Arithmetic average | 1.29 | 0.93 | 0.37 | 0.39 |
| Standard deviation | 0.43 | 0.52 | 0.17 | 0.30 |
| Number of samples | 9 | 9 | 3 | 3 |

on the forest canopy buffered temporal variability of HCOOH in near-surface cloud parcels with which it interacted leading to apparent phase disequilibria based on time-integrated samples. There was evidence for selective depletion of HCOOH relative to CH$_3$COOH in cloud; this depletion was most pronounced at higher pH suggesting HCOOH was rapidly removed by cloud-water deposition. We saw no evidence of significant HCOOH production from the aqueous-phase oxidation of HCHO; it appears that this reaction made at most only a minor contribution to the HCOOH budget at the site.

# References

Atkinson, R., Gas-phase tropospheric chemistry of organic compounds: A review, *Atmos. Environ.*, 24(A), 1-42, 1990.

Bailey, R. G., *Ecoregions of the U.S.*, US Dep. of Agric., Forest Service, Ogden, Utah, 1978.

Betterton, E. A., Henry's law constants of soluble and moderately soluble organic gases: Effects on aqueous phase chemistry, *Adv. Environ. Sci. Technol.*, 24, 1-50, 1992.

Chameides, W. L., and D. D. Davis, Aqueous phase source of formic acid in clouds, *Nature*, 304, 427-429, 1983.

Chao, J., and B. J. Zwolinski, Ideal gas thermodynamic properties of methanoic and ethanoic acids, *J. Phys. Chem. Ref. Data*, 7, 365-377, 1978.

Chin, M., and P. H. Wine, A temperature-dependent competitive kinetics study of the aqueous-phase reactions of OH radicals with formate, formic acid, acetate, acetic acid, and hydrated formaldehyde, in *Aquatic and Surface Photochemistry*, edited by G. R. Helz, R. G. Zepp, and D. G. Crospy, pp. 85-96, Lewis, Boca Raton, Fla., 1994.

Clegg, S. L., and P. Brimblecombe, Solubility of volatile electrolytes in multicomponent solutions with atmospheric applications, in *Chemical Modeling in Aqueous Systems II*, edited by D. C. Melchior and R. L. Brosset, pp. 58-73, American Chemical Society, Washington, D. C., 1990.

Draxler, R. R., Hybrid single-particle Lagrangian integrated trajectories (HY-SPLIT): Version 3.0—User's guide and model description, *NOAA Tech. Memo., ERL ARL-195*, 26 pp., Natl. Tech. Inform. Serv., Springfield, Va., 1992.

Facchini, M. C., et al., Phase-partitioning and chemical reactions of low molecular weight organic compounds in fog, *Tellus*, 44(B), 533-544, 1992.

Galloway, J. N., G. E. Likens, W. C. Keene, and J. M. Miller, The composition of precipitation in remote areas of the world, *J. Geophys. Res.*, 87, 8771-8786, 1982.

Galloway, J. N., W. C. Keene, R. S. Artz, J. M. Miller, T. M. Church, and A. H. Knap, Processes controlling the concentrations of SO$_4^-$, NO$_3^-$, NH$_4^+$, H$^+$, HCOO$_T$ and

CH$_3$COO$_T$ in precipitation on Bermuda, *Tellus, 41*(B), 427-443, 1989.

Gilliam, F. S., J. T. Sigmon, M. A. Reiter, and D. O. Krovitz, Elevational and spatial variation in daytime ozone concentrations in the Virginia Blue Ridge Mountains: Implications for forest exposure, *Can. J. For. Res., 19,* 422-426, 1989.

Graedel, T. E., and T. Eisner, Atmospheric formic acid from formicine ants: A preliminary assessment, *Tellus, 40*(B), 335-339, 1988.

Harrison, E. A., and H. H. Shugart, Evaluating performance of the Appalachian oak forest dynamics model, *Vegetation, 86,* 1-13, 1990.

Jacob, D. J., Chemistry of OH in remote clouds and its role in the production of formic acid and peroxymonosulfate, *J. Geophys. Res., 91,* 9807-9826, 1986.

Jacob, D. J., and S. C. Wofsy, Photochemical production of carboxylic acids in a remote continental atmosphere, in *Acid Deposition at High Elevation Sites,* edited by M. H. Unsworth and D. Fowler, pp. 73-92, Kluwer Academic, Norwell, Mass., 1988.

Jacob, D. J., E. W. Gottlieb, and M. J. Prather, Chemistry of a polluted cloudy boundary layer, *J. Geophys. Res., 94,* 12,975-13,003, 1989.

Johnson, J. J., and E. A. Betterton, Henry's law coefficients for formic and acetic acids, *J. Atmos. Chem.,* in press, 1993.

Joslin, J. D., S. F. Mueller, and M. H. Wolfe, Tests of models of cloud water deposition to forest canopies using artificial and living collectors, *Atmos. Environ., 24*(A), 3007-3019, 1990.

Kawamura, K., L.-L. Ng, and I. R. Kaplan, Determination of organic acids (C$_1$-C$_{10}$) in the atmosphere, motor exhaust, and engine oils, *Environ. Sci. Technol., 19,* 1082-1086, 1985.

Keene, W. C., and J. N. Galloway, Considerations regarding sources for formic and acetic acids in the troposphere, *J. Geophys. Res., 91,* 14,466-14,474, 1986.

Keene, W. C., and J. N. Galloway, The biogeochemical cycling of formic and acetic acids through the troposphere: An overview of current understanding, *Tellus, 40*(B), 322-334, 1988.

Keene, W. C., J. N. Galloway, and J. D. Holden Jr., Measurement of weak organic acidity in precipitation from remote areas of the world, *J. Geophys. Res., 88,* 5122-5130, 1983.

Keene, W. C., et al., An intercomparison of measurement systems for vapor- and particulate-phase concentrations of formic and acetic acids, *J. Geophys. Res., 94,* 6457-6471, 1989.

Lovett, G. M., Rates and mechanisms of cloud water deposition to a subalpine balsam fir forest, *Atmos. Environ., 18,* 361-367, 1984.

Lovett, G. M., A comparison of methods for estimating cloud water deposition to a New Hampshire (U.S.A.) subalpine forest, in *Acid Deposition at High Elevation Sites,* edited by M. H. Unsworth and D. Fowler, pp. 309-320, Kluwer Academic, Norwell, Mass., 1988.

Madronich, S., and J. G. Calvert, Permutation reactions of organic peroxy radicals in the troposphere, *J. Geophys. Res., 95,* 5697-5715, 1990.

McIntyre, B. M., M. A. Scholl, and J. T. Sigmon, A quantitative description of a deciduous forest canopy using a photographic technique, *For. Sci., 36,* 381-393, 1990.

Moody, J. L., A. A. P. Pszenny, A. Gaudry, W. C. Keene, J. N.

Galloway, and G. Polian, Precipitation composition and its variability in the southern Indian Ocean: Amsterdam Island, 1980-1987, *J. Geophys. Res., 96,* 20,769-20,786, 1991.

Munger, J. W., J. Collett Jr., B. Daube Jr., and M. R. Hoffman, Chemical composition of coastal stratus clouds: Dependence on droplet size and distance from the coast, *Atmos. Environ., 23,* 2305-2320, 1989.

Munger, J. W., D. J. Jacob, B. C. Daube, L. W. Horowitz, W. C. Keene, and B. G. Heikes, Formaldehyde, glyoxal, and methylglyoxal in air and cloudwater at a rural mountain site in central Virginia, *J. Geophys. Res.,* this issue.

Pandis, S. N., and J. H. Seinfeld, Should bulk cloud water or fogwater samples obey Henry's law?, *J. Geophys. Res., 96,* 10,791-10,798, 1991.

Pandis, S. N., and J. H. Seinfeld, Reply, *J. Geophys. Res., 97,* 6079-6081, 1992.

Parker, J. G., Throughfall and stemflow in the forest nutrient cycle, *Adv. Ecol. Res., 13,* 57-133, 1983.

Parker, J. G., Evaluation of dry deposition, pollution damage, and forest health with throughfall studies, in *Mechanisms of Forest Response to Acidic Deposition,* edited by A. A. Lancier and S. G. Haines, pp. 10-61, Springer-Verlag, New York, 1990.

Rolph, G. D., R. R. Draxler, and R. G. de Pena, Modeling sulfur concentrations and depositions in the United States during ANATEX, *Atmos. Environ., 26*(A), 73-93, 1992.

Rolph, G.D., R.R. Draxler, and R.G. de Pena, The use of model-derived and observed precipitation in long-term sulfur concentration and deposition modeling, *Atmos. Environ., 27*(A), in press, 1993.

Rutter, A. J., A. J. Morton, and P. C. Robins, A predictive model of rainfall interception in forests, II, Generalization of the model and comparison with observations in some coniferous and hardwood stands, *J. Appl. Ecol., 12,* 367-380, 1975.

Sanhueza, E., and M. O. Andreae, Emission of formic and acetic acids from tropical savanna soils, *Geophys. Res. Lett., 18,* 1707-1710, 1991.

Sanhueza, E., Z. Ferrer, J. Romero, and M. Santana, HCHO and HCOOH in tropical rains, *Ambio, 20,* 115-118, 1991.

Sanhueza, E., M. S. Santana, and M. Hermoso, Gas- and aqueous-phase formic and acetic acids at a tropical cloud forest site, *Atmos. Environ., 26*(A), 1421-1426, 1992.

Schwartz, S. E., Gas-aqueous reactions of sulfur and nitrogen oxides in liquid water clouds, in *SO$_2$, NO and NO$_2$ Oxidation Mechanisms: Atmospheric Considerations,* edited by J. G. Calvert, pp. 173-208, Butterworth, Stoneham, Mass., 1984.

Servant, J., G. Kouadio, B. Cros, and R. Delman, Carboxylic monoacids in the air of Mayombe forest (Congo): Role of the forest as a source or sink, *J. Atmos. Chem., 12,* 367-380, 1991.

Sigmon, J. T., F. S. Gilliam, and M. E. Partin, Precipitation and throughfall chemistry for a montane hardwood forest ecosystem: Potential contributions from cloud water, *Can. J. For. Res., 19,* 1240-1247, 1989.

Talbot, R. W., K. M. Beecher, R. C. Harriss, and W. R. Cofer III, Atmospheric geochemistry of formic and acetic acids at a midlatitude temperate site, *J. Geophys. Res., 93,* 1638-1652, 1988.

Talbot, R. W., M. O. Andreae, H. Berresheim, D. J. Jacob, and

K. M. Beecher, Sources and sinks for formic, acetic, and pyruvic acids over Central Amazonia, 2, Wet season, *J. Geophys. Res.*, *95*, 16,799-16,811, 1990.

Talbot, R. W., B. W. Mosher, B. G. Heikes, D. J. Jacob, J. W. Munger, B. C. Daube, W. C. Keene J. R. Maben, and R. S. Artz, Carboxylic acids in the rural continental atmosphere of the eastern United States during SCAPE, *J. Geophys. Res.*, this issue.

Trumbore, S. E., M. Keller, S. C. Wofsy, and J. M. da Costa, Measurements of soil and canopy exchange rates in the Amazon rain forest using $^{222}$Rn, *J. Geophys. Res.*, *95*, 16,865-16,873, 1990.

Valente, R. J., R. K. A. M. Mallant, S. E. McLaren, R. S. Schemenauer, and R. E. Stogner, Field intercomparison of ground-based cloud physics instruments at Whitetop Mountain, Virginia, *J. Atmos. Oceanic Technol.*, *6*, 396-406, 1989.

Wagman, D. D., W. H. Evens, V. B. Parker, I. Halow, S. M. Bailey, and R. H. Schumm, Selected values of chemical thermodynamic properties, *NBS Tech. Note 270-1*, Natl. Bur. of Stand., Washington, D. C., 1965a.

Wagman, D. D., W. H. Evens, V. B. Parker, I. Halow, S. M. Bailey, and R. H. Schumm, Selected values of chemical thermodynamic properties, *NBS Tech. Note 270-3*, Natl. Bur. of Stand., Washington, D. C., 1965b.

Wagman, D. D., W. H. Evens, V. B. Parker, R. H. Schumm, I. Harlow, S. M. Bailey, K. V. Churney, and R. L. Nuttall, The NBS tables of chemical thermodynamic properties, Selected values for inorganic and $C_1$ and $C_2$ organic substances in SI units, *J. Phys. Chem. Ref. Data, Suppl.*, *11*, 1-392, 1982.

Weast, R. C. (Ed.) *CRC Handbook of Chemistry and Physics*, CRC Press, Boca Raton, Fla., 1979.

Weathers, K. C., et al., Cloud water chemistry from ten sites in North America, *Environ. Sci. Technol.*, *22*, 1018-1026, 1988.

Winiwarter, W., H. Puxbaum, S. Fuzzi, M. M. C. Facchini, G. Orsi, N. Beltz, K. Enderle, and W. Jaeschke, Organic acid gas and liquid-phase measurements on Po Valley fall-winter conditions in the presence of fog, *Tellus 40*(B), 348-357, 1988.

Winiwarter, W., B. Brantner, and H. Puxbaum, Comment on "Should bulk cloud water or fogwater samples obey Henry's law," by S. N. Pandis and J. H. Seinfeld, *J. Geophys. Res.*, *97*, 6075-6078, 1992.

R. S. Artz, Air Resources Laboratory, National Oceanic and Atmospheric Administration, 1325 East-West Highway, Silver Spring, MD 20910.

B. C. Daube, D. J. Jacob, and J. W. Munger, Division of Applied Sciences and Department of Earth and Planetary Sciences, Harvard University, Cambridge, MA 02138.

J. N. Galloway, W. C. Keene, and J. R. Maben, Department of Environmental Sciences, Clark Hall, University of Virginia, Charlottesville, VA 22903.

B. W. Mosher and R. W. Talbot, Institute for the Study of Earth, Oceans, and Space, University of New Hampshire, Durham, NH 03824.